Journal of Power Sources 196 (2011) 2933–2938

Contents lists available at ScienceDirect

Journal of Power Sources

journal homepage: www.elsevier.com/locate/jpowsour

A field operational test on valve-regulated lead-acid absorbent-glass-mat batteries in micro-hybrid electric vehicles. Part II. Results based on multiple regression analysis and tear-down analysis

S. Schaeck[a,*], T. Karspeck[a], C. Ott[a], D. Weirather-Koestner[b], A.O. Stoermer[a]

[a] BMW Group, 80788 München, Germany
[b] ZSW Ulm, 89081 Ulm, Germany

ARTICLE INFO

Article history:
Received 13 June 2010
Received in revised form 30 July 2010
Accepted 29 August 2010
Available online 6 September 2010

Keywords:
Valve-regulated lead-acid battery
Micro-hybrid electric vehicle
Field operational test
Multiple regression analysis
Tear-down analysis

ABSTRACT

In the first part of this work [1] a field operational test (FOT) on micro-HEVs (hybrid electric vehicles) and conventional vehicles was introduced. Valve-regulated lead-acid (VRLA) batteries in absorbent glass mat (AGM) technology and flooded batteries were applied. The FOT data were analyzed by kernel density estimation. In this publication multiple regression analysis is applied to the same data. Square regression models without interdependencies are used. Hereby, capacity loss serves as dependent parameter and several battery-related and vehicle-related parameters as independent variables. Battery temperature is found to be the most critical parameter. It is proven that flooded batteries operated in the conventional power system (CPS) degrade faster than VRLA–AGM batteries in the micro-hybrid power system (MHPS).

A smaller number of FOT batteries were applied in a vehicle-assigned test design where the test battery is repeatedly mounted in a unique test vehicle. Thus, vehicle category and specific driving profiles can be taken into account in multiple regression. Both parameters have only secondary influence on battery degradation, instead, extended vehicle rest time linked to low mileage performance is more serious.

A tear-down analysis was accomplished for selected VRLA–AGM batteries operated in the MHPS. Clear indications are found that pSoC-operation with periodically fully charging the battery (refresh charging) does not result in sulphation of the negative electrode. Instead, the batteries show corrosion of the positive grids and weak adhesion of the positive active mass.

1. Vehicle-assigned field operational test

In the first part of this publication a field operational test (FOT) on VRLA–AGM (valve-regulated lead-acid–absorbent glass mat) and flooded batteries in conventional and micro-HEVs was introduced [1]. The test batteries were operated in test vehicles according to a 'rotational' principle, i.e. a test battery accomplished several test runs in different test vehicles. For practical reasons the organization of such a field test is much easier, but weakens the informative value of the test.

In this paper additional results from a vehicle-assigned FOT are presented (see Fig. 1). Hereby, a unique test battery was assigned to a unique vehicle. The test runs were aimed at a duration of about 6 months. Therefore, if an intermediate analysis (IA) of the battery occurred in the laboratory, the test vehicle was not operated in the meanwhile or equipped with a spare battery. After the lab analysis the battery was re-installed in its test vehicle and the logged data was resetted. This kind of FOT is more elaborate compared to the rotation-based FOT. However, the test design reflects the customer reality in a better way and the impact of vehicle-specific peculiarities, e.g. configuration of additional equipment or special driving profiles, may also be detected.

Some further boundary conditions have to be introduced:

(a) *Driving profile*: Four fleets of the FOT were introduced in part I of this publication [1]. Here, mainly pre-series vehicles and VIP shuttle-service vehicles were involved. The pre-series vehicles were operated with specific driving profiles. These were an urban profile, a highway profile and a mixed profile with city, overland and highway parts. It has to be noted that these vehicles were operated in two to three shifts per day for endurance

Abbreviations: AGM, absorbent glass mat; C_{act}, actual 20 h-capacity (maximum available capacity); C_{nom}, nominal 20 h-capacity; COT, customer-oriented test; CPS, conventional power system; DF, degree of freedom; fc, full cycle; FOT, field operational test; HEV, hybrid electric vehicle; LA, lead-acid; MHPS, micro-hybrid power system; NAM, negative active mass; NE, negative electrode; PAM, positive active mass; PE, positive electrode; pSoC, partial state-of-charge; R^2, coefficient of determination; R^2_{adj}, adjusted coefficient of determination; SoC, state-of-charge; TDA, tear-down analysis; VRLA, valve-regulated lead-acid.

* Corresponding author. Tel.: +49 89 382 78653; fax: +49 89 382 42827.
E-mail address: stefan.schaeck@bmw.de (S. Schaeck).

0378-7753/$ – see front matter © 2010 Elsevier B.V. All rights reserved.
doi:10.1016/j.jpowsour.2010.08.101

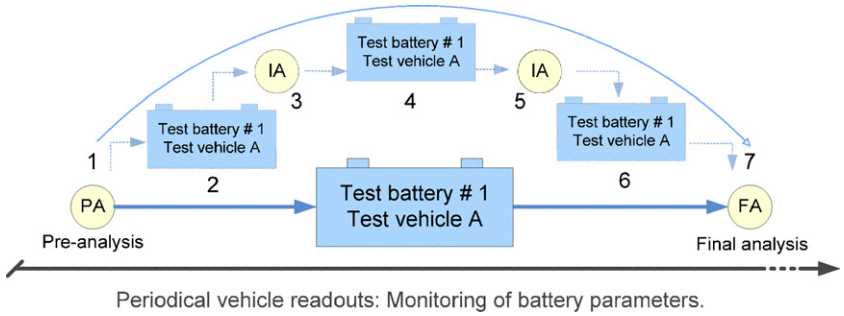

Fig. 1. Vehicle-assigned FOT: A test battery is exclusively operated in one specific vehicle. Intermediate electrical analysis in the laboratory was accomplished.

testing. As a result the average annual mileage and battery cycling was exceptionally high at low calendar age. Additional equipment was possibly used intensively. In contrast, the cycling rate per mileage tended to be underrepresented due to little proportions of short trips, rest times and pre- and post drive phases. Therefore, a fourth driving profile was made part of the vehicle-assigned FOT. This is a customer-oriented test profile (COT), i.e. vehicle rest periods, short trips and mixed road profiles are considered. This driving profile was comparable to the driving profile of the VIP shuttle-service cars in the rotation-based FOT in [1].

(b) *Vehicle categories*: The vehicle-assigned FOT was not only used for a differentiation of driving profiles, but also different vehicles categories. Four fundamental categories were involved, which were the compact class (e.g. MINI cars, BMW 1 series), the mid class (e.g. BMW 3 series), the upper class (e.g. BMW 5 series) and the luxury class (BMW 7 series).

(c) *Battery types*: VRLA–AGM batteries (70, 80, and 90 Ah) were either assigned to vehicles with micro-hybrid power system (MHPS) or conventional power system (CPS). A few battery samples were flooded batteries (90 and 110 Ah) and operated only in CPS cars (12%). Batteries from four different manufacturers were used. The batteries were either released or in the approval process. The manufacturers are anonymised in this publication.

(d) *Info recorder information*: Following parameters based on info recorder entries were used for data evaluation: Cycling per mileage, mileage performance, relative operational hours in SoC range and relative operational hours in temperature range.

As described in part I of the publication, all available information from vehicle test runs and laboratory measurements was collected in a data base [1]. In the following, batteries from both FOT test designs are regarded by the use of multiple regression analysis.

2. Multiple regression analysis

Various parameters may influence battery degradation like battery technology, manufacturer and design, vehicle category, power net and operational conditions. A variation of these parameters is represented by the FOT. Battery degradation was detected by electrical measurement. Therefore, relevant information was collected in the data base in order to quantitatively investigate correlations between battery degradation and battery application: Which parameters have the greatest influence on the operational behaviour of batteries in vehicles? Has, e.g. the driving profile a stronger impact on the capacity loss of a VRLA–AGM battery than if the battery supplies the MHPS or the CPS?

Such a problem is mathematically investigated by the method of multiple linear regression [2,3]. According to common literature, a comparable analysis of LA batteries in automotive application was not reported before. The FOT data structure was subject to a multiple regression model, which was implemented by use of the data analysis tool 'Visual-XSel' by CRGRAPH [4,5]. The relative capacity loss was chosen as dependent variable, several of the above introduced parameters were chosen as independent variables. The linear regression model was designed as square model with n independent parameters and m measured values according to:

$$\hat{y} = c_1\hat{x}_1 + \cdots + c_n\hat{x}_n + c_{n+1}\hat{x}_1^2 + \cdots + c_{2n}\hat{x}_n^2 + \hat{\varepsilon}$$

or for $i = 1, .., m$: $y_i = c_1x_{1,i} + c_2x_{2,i} + \cdots + c_nx_{n,i} + c_{n+1}x_{1,i}^2 + c_{n+2}x_{2,i}^2 + \cdots + c_{2n}x_{n,i}^2 + \varepsilon_i$ respectively, with $\hat{y}$ as the regression value of the capacity loss, y_i as its measured values, $\hat{x}_j$ as the n regression values of the independent parameters, e.g. mileage performance, $x_{j,i}$ as their measured values, $\hat{\varepsilon}$ as the error of the model, and ε_i as the measured residual. Square terms in the model are especially advantageous if the independent parameters are not normally distributed in the basic data population [5,6].

Intercorrelations of the independent parameters like $c\hat{x}_k\hat{x}_j$ with $j \neq k$ were not regarded in the model. Originally, such a model was considered, however, no additional knowledge could be gained. The vector of coefficients $(c_1,\ldots,c_{2n})$ is calculated by the method of least-squared errors. The presented figures in the next section show these coefficients c_j for the parameters $\hat{x}_j$, which were identified as significant in the model. This significance is given by the p-value. The significance level was set to 5%, i.e. p-values $\leq$0,05 were requested. Furthermore, a 90% confidence interval is given for the target value $\hat{y}$. Also the processing of outliers in the regression analysis has to be commented. These are typically found by their residuals and are subject to the Grubb's test for outliers, a standard test in probability theory [7,8]. 'Visual XSel' applies this method for identification of outliers and recalculates the model after elimination [5].

3. Results and discussion

In this section the main results of the multiple regression analysis are presented. In Figs. 2 and 3 the relative capacity loss per cycling rate is shown for the rotation-based FOT. The x-axes depict the significant independent variables of the regression model. Capacity loss is given as function of these independent parameters on the y-axis, which is determined by the coefficients c_n. A reference regression value is given for the target value and the independent variables by the red lines. It shows that the capacity improves by 6% per 10 fc (ref. to C_{nom}) if an AGM battery of type #1 is mounted in a MHPS vehicle with a cycling rate accounting for 408 fc/1000 km and a mileage performance of 310 km d^{-1}. The high cycling rate and the high mileage per day represent the weakness of the data sets. The pre-series vehicles used for this analysis were intensely operated as mentioned above and in part I [1]. Especially, longer vehicle rest periods were underrepresented. Furthermore, it has to be reminded that the batteries were of good condition before mounting into the

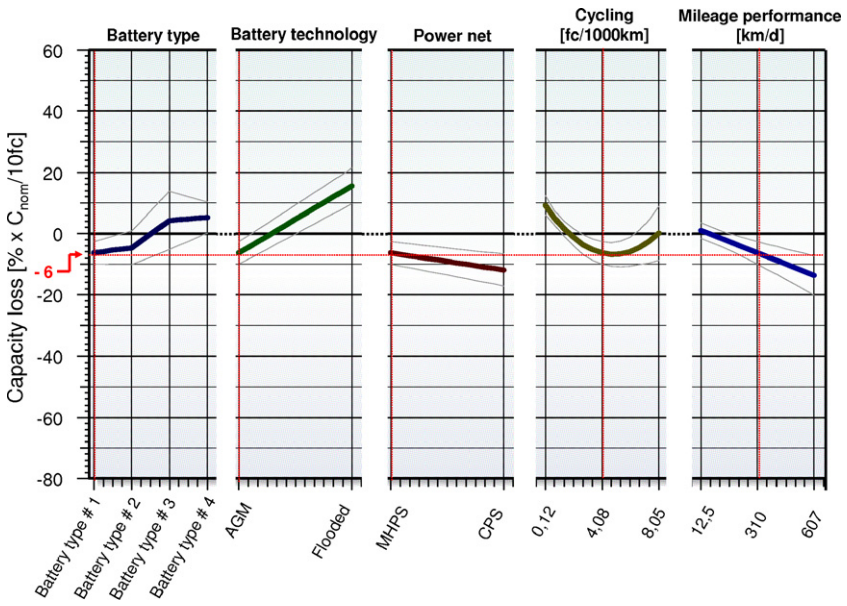

Fig. 2. Multiple regression analysis of the capacity loss. Only significant parameters are depicted (p-value ≤ 0.05). The adjusted coefficient of determination is $R^2_{adj} = 67\%$ ($R^2 = 71\%$) at a degree of freedom of 142. The given confidence intervals are 90%.

test vehicle and the test runs did not mark the end of life scenarios due to scheduled dismounting. This means that 'only' the initiation of battery wearing is presented. Therefore, this type of experiment is appropriate for describing impacts on battery degradation and its correlations, but not for stating quantitatively accurate failure predictions. Also the term battery improvement has to be shortly discussed: In the rotation-based FOT it may happen that an aged battery accomplishes a higher C_{act} after a test run than before the test run. In Figs. 2 and 3, where capacity differences of test runs are evaluated, this is depicted as 'negative' capacity loss. Furthermore, it has to be mentioned that the initial capacity C_{ini} of brand-new batteries is usually 5% higher than C_{nom}. If the measured C_{20}-values of the FOT are referred to C_{ini} instead of C_{nom}, the results of the experiment do not change qualitatively.

The relative dependencies of influencing factors are made visible by multiple regression analysis: If, for example, all significant parameters would have been kept constant, but the test battery would have been supplied by manufacturer #3, the model would have expected a 5% capacity loss per 10 fc under the given conditions instead of 6% capacity improvement with manufacturer #1. Interestingly, both the absolute calendar age and the absolute number of operated full cycles were identified as insignificant parameters in the model (therefore not listed in Figs. 2 and 3). These parameters are implicitly described by the variables 'mileage performance' and 'cycling rate'.

The precision of a multiple regression model is given by the adjusted coefficient of determination R^2_{adj} better than by R^2 as it adjusts to the number of explanatory terms of the model [5]. This value displays to what extent the measured scattering is explained by the model. Both the degree of freedom (DF, ensemble size minus explanatory terms in the model) of the model in Figs. 2 and 3 (DF = 142) and the residuals from the least-square-optimisation

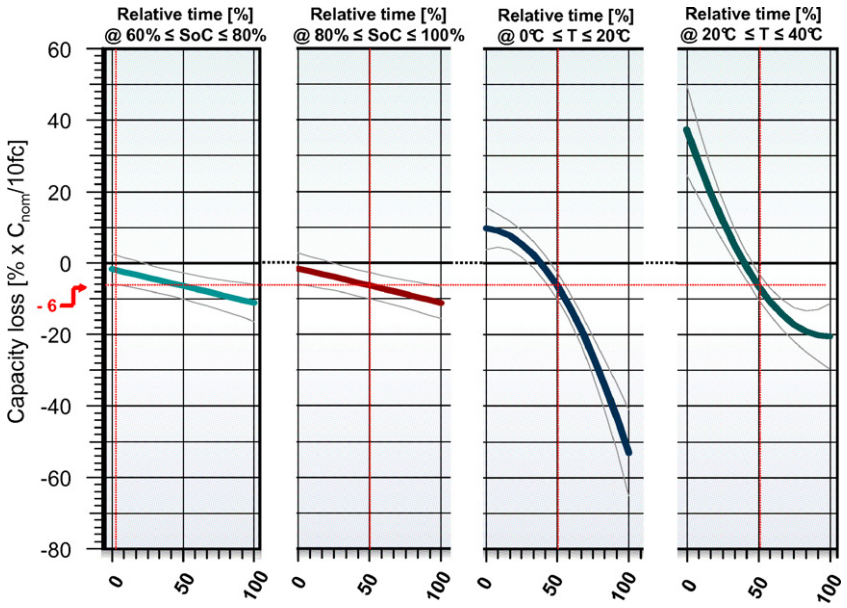

Fig. 3. Part II of the regression model given by Fig. 2. The coefficients show that temperatures above 40 °C and below 0 °C induce strong degradation of lead-acid batteries.

contribute to R^2_{adj}. The presented model has an adjusted coefficient of determination of $R^2_{adj} = 67\%$ ($R^2 = 71\%$). On the base of the complexity of the FOT, this value can be considered as very satisfactory.

The following main statistical effects can be derived from Fig. 2:

- Flooded batteries are considerably worse than AGM batteries regarding capacity loss. According to [1] this is caused by acid stratification.
- This effect dominates the influence of power net technology. At the current development stage of AGM batteries and the MHPS, the negative influence of pSoC-operation on the degradation of AGM batteries is almost negligible if the reference is a flooded battery operated at full SoC (the standard configuration for decades in the automotive industry).
- However, it is observed that the best configuration is operating a VRLA–AGM battery in the CPS. The negative slope of capacity loss across the third abscissa (vs. power net) would be even steeper towards the CPS if flooded batteries would have been excluded from the regression model.
- There is a quite high degree of scattering between batteries from different manufacturers. The maximum difference referred to capacity deltas between manufacturer #1 and manufacturer #4 is $12\%{\cdot}C_{nom}/10$ fc. It was found in [9] that the most crucial parameters of AGM batteries for pSoC-operation are the degree of saturation of the separator with electrolyte, the plate stack pressure and the ratio of active masses. The impact induced by the battery manufacturer exceeds the influence of the power net technology.
- Low mileage performance is detrimental in terms of capacity loss. It is linked to short trip travelling and/or extensive vehicle rest time. Both effects favour charge depletion of the battery because of a negative charge balance and/or worse charge acceptance, see also [10].
- An extremely high cycling rate causes enhanced battery degradation. As high cycling per mileage is correlated to a high absolute fc number, this phenomenon is inherent to battery wearing.
- Extremely low cycling rates tend to be disadvantageous as well. This behaviour is not yet fully understood. A possible explanation for this trend may be the fact that the capacity loss is referred to the number of full cycles in Fig. 2. In this case a high mileage has to be reached in order to complete an absolute number of full cycles, e.g. 10 fc like in Fig. 2. If the same mileage performance is assumed (regression model without correlation of the independent parameters), higher calendar age is linked to the batteries with low cycling rate (in fc/1000 km) compared to batteries with higher cycling rate at a comparable absolute number of full cycles. Therefore, two aspects have to be regarded, if the batteries with lower cycling rate reveal higher capacity loss like in the presented experiment: These batteries tend to have higher calendar age and higher mileage at a specific number of full cycles and age in fact 'slower' if capacity loss is referred to calendar age or mileage. The latter aspect corresponds to the more common picture of battery aging and is supported by the vehicle-assigned FOT (see Fig. 4, right abscissa): The batteries with the highest cycling rate lose most capacity (per mileage).
- In terms of cycling the lowest capacity loss is found in the mid of the represented range, i.e. at about 4.5 fc/1000 km. It has to be pointed out that the absolute numbers have to be interpreted conditionally because of the FOT characteristics (see Section 1).

Fig. 3 shows the second part of the regression model. The temporal distributions of SoC and temperature during battery operation were found as quite significant parameters (p-values ≤ 0.01). It has to be noted that both parameters were available in the form of histograms in the onboard monitoring system. Each bin was introduced as independent parameter to the model. Indeed, it has to be mentioned that these parameters are implicitly dependent of each other. For example, if the battery is not operated in the range $80\% \leq SoC \leq 100\%$ the other SoC-related bins (e.g. $60\% \leq SoC \leq 80\%$) are automatically affected by higher probability. However, this fact is also useful for interpretation of the results in Fig. 3. It was found that there is the less capacity degradation the more the battery is operated in the range $60\% \leq SoC \leq 100\%$ (left two abscissas in Fig. 3). The reverse interpretation is valid: More capacity loss was detected when operation occurred with focus in $0\% \leq SoC \leq 40\%$. Of course, this conclusion is not surprising as it meets the common expectation of LA batteries. However, the more interesting interpretation from Fig. 3 concerns the comparison with temperature distribution. Capacity loss is especially found when the time share of battery operation in the temperature ranges $0\,^\circ C \leq T \leq 20\,^\circ C$ and $20\,^\circ C \leq T \leq 40\,^\circ C$ converges to zero (in a temporal temperature histogram of battery operation). Thus, if the battery is operated most of the time out of the $0\,^\circ C \leq T \leq 40\,^\circ C$ range, most tremendous capacity loss occurs. Also this result is qualitatively not surprising and was, e.g. also not long ago described by Soria et al. by the example of spiral-wound lead-acid batteries with the insight that higher performance loss was found at elevated working temperature of the battery [11]. However, it can be directly concluded from the FOT that it is by a factor of 3–4 more harmful for a LA battery if it is operated in an inappropriate temperature range (outside $0\,^\circ C \leq T \leq 40\,^\circ C$) instead of an inappropriate SoC range (outside $60\% \leq SoCT \leq 100\%$). This demonstrates that influencing input parameters can be assessed relatively to each other under realistic operational conditions by the multiple regression analysis.

A separate multiple regression model was implemented for the vehicle group, which was operated in the vehicle-related FOT with pre-series vehicles (see Section 1). It is depicted in Fig. 4. The unique characteristic of this model is the input parameters 'vehicle category' and 'driving profile'. All of the vehicles were equipped with VRLA–AGM batteries operated at pSoC. Again, a square model without mixed terms of independent parameters was used. The adjusted coefficient of determination accounted for only $R^2_{adj} = 45\%$ ($R^2 = 58\%$). This comes from the complexity of the tested system and from the low number of samples (DF = 52). However, the special test conditions (particular vehicle category with a particular driving profile) are difficult to realize with statistical significance.

In Fig. 4 the vehicle category is depicted although it was not found as significant parameter (p-value >0.05). It is seen also from the 90% confidence level (black thin lines) that it is irrelevant for the relative capacity loss if 5000 km are driven in a compact or in a luxury car. It has to be noted that this does not hold true for the absolute capacity loss as larger batteries are installed in larger vehicles. This insight indicates that the onboard energy management performs well and that the system design vehicle/battery is appropriate. In contrast, the driving profile was found as significant parameter, however, the main influence is given by the 'highway' profile. Then, high mileage is reached in short time and the alternator is coupled to sufficient rotational speed at any operating point. At COT conditions capacity loss seems to be slightly increased, which is most probably linked to longer rest periods. This result shows correlation with the observed dependence on mileage performance. High mileage performance (mainly the highway vehicles) results in even slight capacity growth. However, low mileage performance is associated by enhanced capacity loss. Two aspects are linked to this result: Firstly, as capacity loss is normalised to mileage in Fig. 4, mileage performance behaves inversely to the absolute calendar age. Secondly, longer rest times affect the battery negatively especially at pSoC-operation (see [10]), which was already observed and discussed in Fig. 2. This is the major motivation for implementation of a battery refresh function. Nevertheless, the refresh function is not able to totally eliminate the negative effect of long vehicle rest

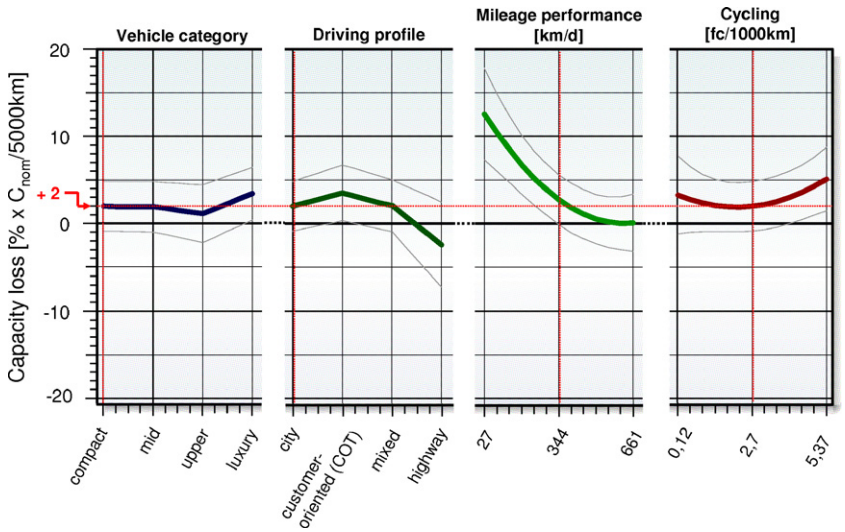

Fig. 4. Multiple regression model based on data from the 'vehicle-assigned' field test. The capacity loss is related to the absolute mileage because particular driving profiles are of interest. The coefficients of the square model (R^2_{adj} = 45%, DF = 52, R^2 = 58%) predict that the mileage per day, i.e. mileage performance, has a larger influence than the vehicle category or the particular driving profile.

time and/or negative charge balance of the battery. In this context the potential of high-carbon negative plates has to be mentioned, which is described by Moseley et al. [12]. When the concentration of carbon in the NAM is raised to several weight percent, it is expected that sulphation effects might be minimized or even eliminated [12]. The exact mechanisms related to carbon additives in the negative plate are not yet fully understood and subject of promising ongoing research, which is fundamental for implementation in standard products of battery manufacturing [13,14]. An even further development step aims at the combination of a negative carbon-based negative plate with a PbO_2 positive plate in on cell, known as Ultrabattery [15]. It is reported by Lam et al. that this concept of a hybrid energy storage device is able to introduce positive aspects of supercapacitors to the lead-acid technology resulting in higher cycling performance and a wider SoC window for pSoC-operation [15].

It is also clearly shown by Fig. 4 that mileage performance has the most serious influence on capacity loss. The influence of cycling was already discussed in the context of Fig. 2.

4. Tear-down analysis of FOT batteries

Four batteries, which were operated in the FOT in micro-HEVs, were randomly selected for a TDA (tear-down analysis, see Table 1, samples 'T01'–'T04'). A VRLA–AGM battery operated in the CPS with high cycle number served as a reference (sample 'T0R'). All batteries are from the same manufacturer (#1 in Fig. 2). The TDA included a quantitative analysis of the $PbSO_4$ content of the active masses by titration analysis. It was found that sulphation of the negative active mass (NAM) cannot be identified as dominating aging phenomenon. One of the batteries (sample 'T03') revealed extreme $PbSO_4$ content at the bottom of the electrodes. This effect correlates with decreased liquid mass ratio of the separator. It is discussed in [9,16] that pSoC-operation was expected to be the main root cause for battery aging by inducing hard sulphation of the NE as introduced by, e.g. [17]. Instead, corrosion of the positive grid and adhesion of the PAM were found as the main degradation phenomena of pSoC-operated batteries (Fig. 5a). In contrast, the reference sample 'T0R', which was operated in the CPS up to 173 fc, showed only weak grid corrosion and intact PAM. Here the NE reveals initiation of hard sulphation across the entire surface, which was approved by scanning electron micrographs (Fig. 5b). Actually, this behaviour might have been expected from pSoC-operation. Sample 'T02' suffers from stronger capacity loss with otherwise similar parameters. This shows exemplary the scattering effect of field test batteries as demonstrated in [1]. Unlike it was reported from flooded lead-acid batteries in pSoC-operation corrosion of the negative plate lugs was not an issue [18].

Of course, the sample size of five teared-down batteries may only give tendencies and is not representative for the entire FOT. However, the conclusions of the presented TDA are supported by a publication in 2007. Road tests in the Kyoto area, Japan, with VRLA–AGM batteries mounted in idling-stop vehicles were reported by Sawai et al. [19]. Operation at pSoC and a battery refresh charge, termed as equalizing charge, were applied, too. Like in the presented FOT, corrosion of the positive grid was identified as main aging mechanism by Sawai and co-workers. This gives

Table 1
Results of battery tear-down analysis. Four batteries operated in the MHPS and a reference battery operated in the CPS were selected. Mass% percentage of $PbSO_4$ was determined by titration analysis. The liquid mass ratio of the separator material was measured by an evaporization method. The value of ≈83% for a brand-new reference battery with this technique corresponds to ≈95% degree of saturation of the AGM material with electrolyte.

Battery sample	T01	T02	T03	T04	T0R
Power net	MHPS	MHPS	MHPS	MHPS	CPS
Mileage [tkm]	146	214	180	196	152
Full cycles [–]	–	114	96	–	173
C_{act} [Ah]	66.3	37.4	79.3	57.3	91.7
PAM $PbSO_4$-content [mass%]					
Top	9.9	11.1	14.2	8.9	6.4
Mid	10.2	10.6	17.9	9.6	6.8
Bottom	10.0	12.6	30.1	15.1	8.7
PE corrosion	Strong	Strong	Strong	Strong	Weak
NAM $PbSO_4$ content [mass%]					
Top	6.2	6.9	7.7	8.1	16.5
Mid	5.6	7.6	6.3	7.1	30.0
Bottom	15.7	9.2	48.0	17.6	39.1
Liquid ratio of separator [mass%]					
Top	79.1	79.8	76.9	81.8	80.9
Mid	7S.7	78.7	77.7	81.5	81.0
Bottom	79.8	79.5	78.4	81.3	80.5
Acid density [g cm^{-3}]					
Top	1.31	1.32	1.25	1.28	1.29
Mid	1.32	1.31	1.27	1.30	1.29
Bottom	1.31	1.30	1.27	1.31	1.30

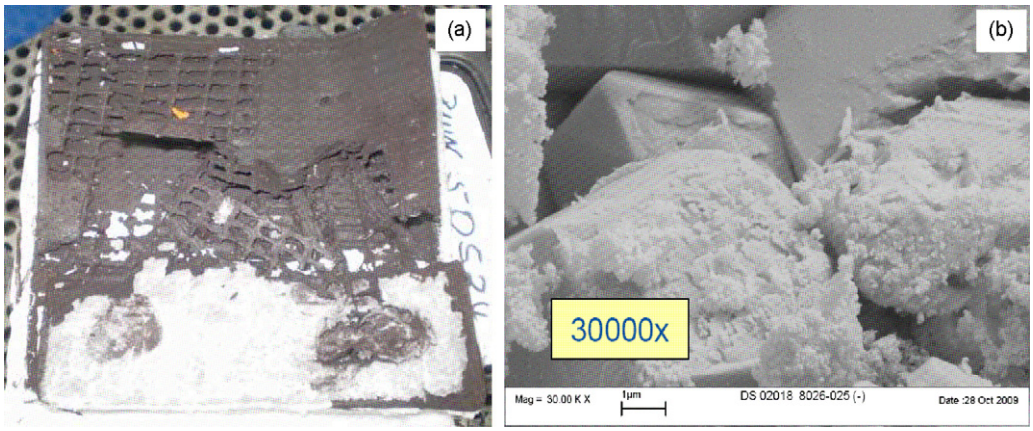

Fig. 5. (a) Positive plate of sample 'T03'. The detected degree of grid corrosion and lack of positive active mass adhesion is representative also for the other MHPS batteries of Table 1. (b) Electron scanning micrograph of the negative active mass of the reference sample 'T0R'. First signs of hard sulphation could be found as lead sulphate crystal diameters reached 5–10 μm maximum.

rise to the conclusion that the refresh function effectively disables hard sulphation in real-life application (and not only bench test experiments, see [16]). Thus, limited battery life time results in the fact that other aging phenomena are more prominent. Due to the increased maximum voltage level (maximum 14.8 V, temperature-independent) and the charge factor larger than 1 of the refresh function [9], PE grid corrosion may be favoured. Nevertheless, it has to be stated that associated battery degradation is much more moderate than, e.g. for flooded batteries in the CPS and for VRLA–AGM batteries operated in the MHPS without any refreshing [7,16].

5. Summary

A field operational test was analyzed by the means of multiple regression analysis. It aimed at phenomenological degradation of LA batteries in automotive application, which was detected by the loss of capacity. It was found with a square regression model that the highest rate of capacity loss is caused if LA batteries are operated outside $0\,^{\circ}C \leq T \leq 40\,^{\circ}C$. Low SoC and long rest time were identified as serious influence parameters as well. Furthermore, it was proven that VRLA–AGM batteries operated at pSoC in the MHPS are considerably less affected than flooded batteries in the CPS. Permanently targeted full SoC like in the CPS was detected as advantageous also for VRLA–AGM batteries, but was of subordinate relevance in the experiment. The scattering of battery durability between different manufacturers had an at least comparable impact.

A multiple regression model based on data stemming from a vehicle-related FOT was also discussed. It could be demonstrated that the influence of vehicle categories and driving profiles is secondary compared to the absolute mileage performance. Low mileage performance induces longer vehicle rest periods and short trips with negative charge balance, which initiates battery degradation. Tear-down analysis provided information about the mechanisms of battery aging in the MHPS. This was mainly corrosion of the positive grid and diminished adhesion of the positive active mass.

Acknowledgements

We gratefully thank C. Ronniger for Visual-XSel support and H. Koch (Combatec GmbH) for constructive cooperation with TDA.

References

[1] S. Schaeck, T. Karspeck, C. Ott, M. Weckler, A.O. Stoermer, A field operational test on VRLA–AGM batteries in micro-hybrid electric vehicles. Part I. Results based on Kernel Density Estimation, Journal of Power Sources, accepted manuscript.
[2] L. Fahrmeir, R. Künstler, I. Pigeot, G. Tutz, Statistik–Der Weg zur Datenanalyse, Springer-Verlag, Berlin, 2007.
[3] R.H. Myers, Classical and Modern Regression with Applications, Brooks/Cole, 1990.
[4] CRGRAPH, http://www.crgraph.de, last call 04/2010.
[5] C. Ronniger, Versuchsmethoden Statistik & DoE, Auflage 10d, 2007, www.versuchsmethoden.de.
[6] H. Wilker, Systemoptimierung in der Praxis, Teil 1–Leitfaden zur statistischen Versuchsauswertung (Band 1), Books on Demand, Norderstedt, 2006.
[7] J. Hartung, B. Epelt, K.H. Klösener, Statistik - Lehr- und Handbuch der angewandten Statistik, Oldenbourg, 2005.
[8] F.E. Grubbs, Sample criteria for testing outlying observations, Annals of Mathematical Statistics 21 (1950) 27–58.
[9] S. Schaeck, Simultaneous engineering-based investigation of VRLA–AGM batteries in micro-hybrid electric vehicles, PhD Thesis, Universität Ulm, submitted for publication.
[10] S. Schaeck, A.O. Stoermer, F. Kaiser, L. Koehler, J. Albers, H. Kabza, Lead-acid batteries in micro-hybrid applications. Part I. Selected key parameters, Journal of Power Sources 196 (2011) 1541–1554.
[11] M.L. Soria, F. Trinidad, J.M. Lacadena, A. Sánchez, J. Valenciano, Journal of Power SourcesV 168 (2007) 12–21.
[12] P.T. Moseley, R.F. Nelson, A.F. Hollenkamp, Journal of Power Sources 157 (2006) 3–10.
[13] D. Pavlov, T. Rogachev, P. Nikolov, G. Petkova, Journal of Power Sources 191 (2009) 58–75.
[14] P.T. Moseley, Journal of Power Sources 191 (2009) 134–138.
[15] L.T. Lam, R. Louey, N.P. Haigh, O.V. Lim, D.G. Vella, C.G. Phyland, L.H. Vu, J. Furukawa, T. Takada, D. Monma, T. Kano, Journal of Power Sources 174 (2007) 16–29.
[16] S. Schaeck, A.O. Stoermer, E. Hockgeiger, Journal of Power Sources 190 (2009) 173–183.
[17] P.T. Moseley, Journal of Power Sources 127 (2004) 27–32.
[18] T. Takeuchi, K. Sawai, Y. Tsuboi, M. Shiota, S. Ishimoto, N. Hirai, S. Osumi, Journal of Power Sources 189 (2009) 1190–1198.
[19] K. Sawai, T. Ohmae, H. Suwaki, M. Shiomi, S. Osumi, Journal of Power Sources 174 (2007) 54–60.